JOURNAL OF CATALYSIS 54, 31–41 (1978)

Infrared Study of CO_2 Adsorption on SiO_2

A. UENO AND C. O. BENNETT

Department of Chemical Engineering, University of Connecticut, Storrs, Connecticut 06268

Received June 23, 1977; revised March 8, 1978

The adsorption of CO_2 on SiO_2 was studied by means of infrared spectroscopy. The desorption of CO_2 is accounted for by the assumption of two kinds of adsorbed species of CO_2 on SiO_2. By adsorption measurements after modification of the surface OH groups on SiO_2 by heat treatments, it was deduced that these two adsorbed CO_2 species are related to the isolated surface OH groups (which have an absorption band at 3750 cm^{-1}) and the bonded OH groups (which have a broad band centered at 3550 cm^{-1}), respectively. The isosteric heats of adsorption and the activation energies for desorption were calculated for both CO_2 adsorbed species. They are 5.0 and 5.2 kcal/mol, respectively, for CO_2 adsorbed on isolated OH groups, and 5.1 and 5.0 kcal/mol for bonded OH groups. The changes in the standard entropies of adsorption are also discussed in relation to the structure of CO_2 hydrogen-bonded to the OH groups; the CO_2 adsorbed on the bonded OH groups has a higher entropy than that adsorbed on the isolated OH groups.

INTRODUCTION

One of the aims of the application of infrared spectroscopy to the study of catalysis is to identify the properties of active sites on the surface of a catalyst. Many studies have been done on the surface hydroxyl groups of oxide catalysts (*1–4*) and of zeolite catalysts (*5*). Elegant experiments were introduced by Peri (*6*) to identify the geometrical locations of the surface hydroxyl groups on Al_2O_3 by means of infrared spectroscopy. According to his results, infrared absorption bands depended not only on whether OH groups were isolated or bonded by hydrogen bonding but also on the numbers of O^{2-} ions surrounding isolated OH groups of the Al_2O_3 surface. The five adsorption bands observed were assigned to the isolated OH groups according to the O^{2-} ion concentrations. For SiO_2, its OH groups have so far only been separated into the isolated and bonded groups (*7*). Thus, there should be only one absorption band assigned to the isolated OH group on SiO_2. It has been usually observed at 3747 cm^{-1}, and the bonded OH group is centered at approximately 3500 cm^{-1}.

The surface states of the oxide catalysts, and, in particular, those associated with OH groups, are by now quite well understood. Their reactivities, however, are still ambiguous. In order to study this question, the adsorption of gases onto oxides has been investigated (*8*, *9*) by infrared techniques. Carbon dioxide (*10*, *11*) has been used as one of these adsorbates in order to test ideas on the acid–base concept of catalysis.

Usually, carbon dioxide adsorbs on metal catalysts to form the carboxylate ion (*12*) and adsorbs on oxygen atoms of oxide catalysts to produce the carbonate ion (*13*). Eischens (*14*) was the first to observe the molecular state of CO_2 adsorption when CO_2 was added to SiO_2 catalyst at

0021-9517/78/0541-0031$02.00/0

room temperature. This adsorbed CO_2 was observed to be free from its rotation, but its absorption band appeared at a wave number very close to that of gaseous CO_2. This was the basis of assigning the band to physisorbed CO_2 on SiO_2. Since Eischens' observations on the molecular state of CO_2 adsorption, there have been several papers reporting the same adsorption on Al_2O_3 (*15*) and on Ag supported on SiO_2 (*16*). However, less attention was paid to this adsorption because of its assignment to the physisorbed species.

Recently, Conner and Bennett (*17*) observed oxygen exchange between $C^{18}O_2$ and SiO_2 at 180°C, which means that CO_2 chemisorbed on SiO_2. Peri (*18*) also observed this oxygen exchange on SiO_2 at higher temperature. According to his results, CO_3^{2-} was proposed as the intermediate of this exchange reaction. The absorption bands corresponding to CO_3^{2-} on SiO_2 were not observed, however, when CO_2 was added. The observed weak band corresponded to adsorbed molecular CO_2.

In the case of Al_2O_3, Parkyns (*19*) observed adsorbed molecular CO_2, and it was also assigned to physisorbed CO_2. Its intensity in the spectrum increased with elevated preheating temperatures, however, and this caused a decrease in the surface area of Al_2O_3. If this is physisorption, its intensity should decrease with the reduction of the surface area of Al_2O_3.

The purpose of the present work is to obtain information concerning the molecular-type adsorbed CO_2 on SiO_2 as a function of the surface OH states. The dynamic transient technique, developed by Kobayashi and Kobayashi (*20*) and one of the present authors (*21*), was applied for the analysis of the transient of CO_2 desorption.

EXPERIMENTAL

The measurements were carried out in a flow system associated with an infrared

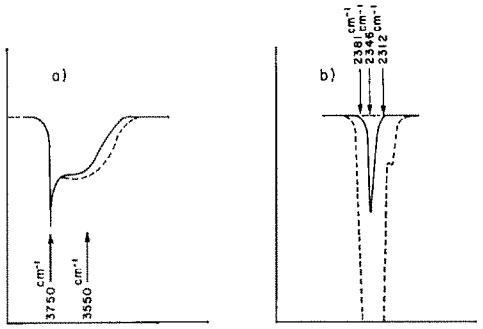

FIG. 1. (a) Infrared spectrum of OH groups on SiO_2 at 31°C (SiO_2 was preheated at 150°C): (– – –) in the presence of CO_2; (——) approximately 3 min after flushing CO_2 by Ar. (b) Infrared spectrum of absorbed CO_2 on SiO_2: (– – –) in the presence of CO_2; (——) approximately 3 min after flushing CO_2 by Ar.

spectrometer (Spex 1701, Harrick) with optics the same as reported previously (*22*). The reactor cell used was also the same, except that BaF_2 was used as an infrared window instead of Irtran 6. The window made of BaF_2 allowed us to keep the reactor at temperatures higher than 300°C. The spectroscopic conditions employed were as follows: To obtain the usual spectrum, the physical slit widths were 1.25 mm, and the time constant was 0.3 sec, with a sensitivity of 250 μV on the lock-in amplifier (P.A.R. Model 128). To follow the change in the transmission during CO_2 desorption, the wavenumber to be measured was fixed at the maximum absorption position of the band due to CO_2 adsorbed (invariant with intensity), and the signal was recorded with a sensitivity of 100 μV and a time constant of 0.1 sec. The changes with time of both sides of the band were also recorded at 2381 and 2312 cm^{-1} for every experimental run. The optical density was calculated every 5 sec by using these three wavenumbers.

Carbon dioxide desorption was performed by the replacement of a given CO_2 atmosphere in the reaction cell by Ar, i.e., by the quick switching to Ar flow from CO_2

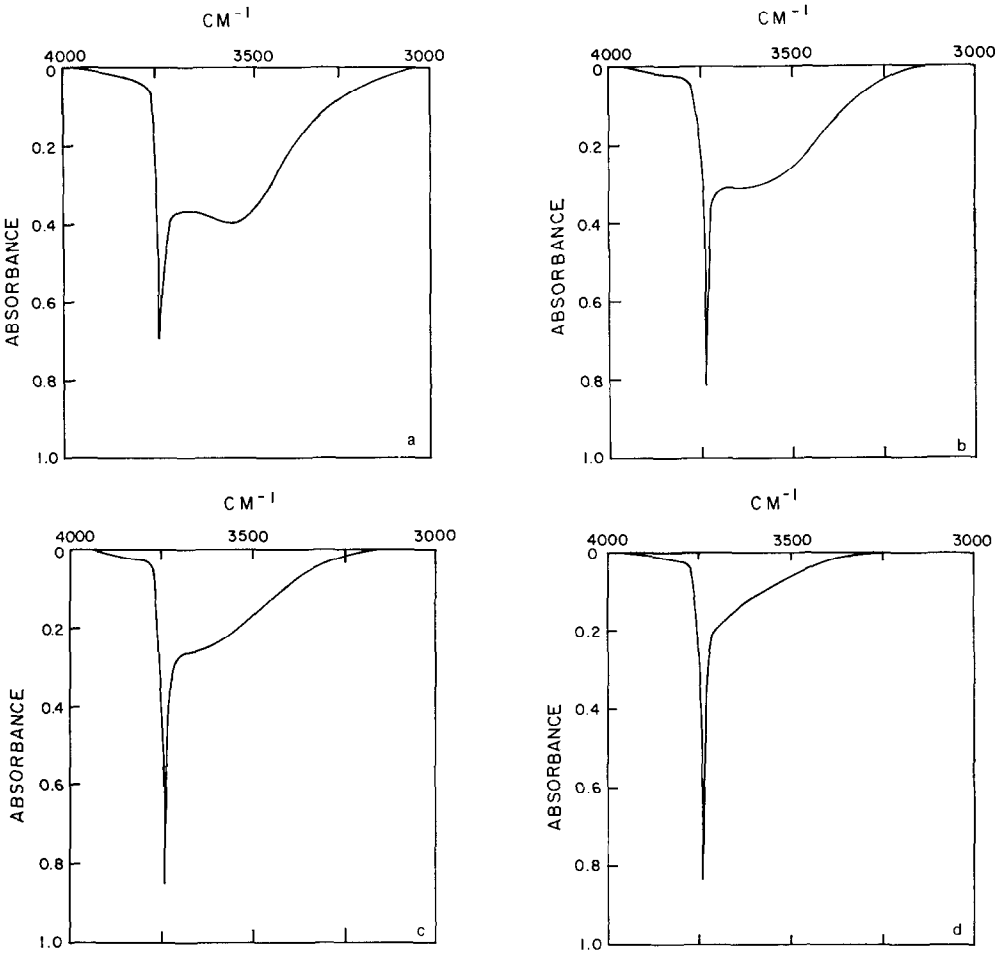

FIG. 2. Infrared spectrum of OH groups on SiO_2 varied by heat treatment: (a) original SiO_2; (b) preheated at 150°C for 4 hr in Ar; (c) preheated at 200°C for 5 hr in Ar; (d) preheated at 350°C for 5 hr in Ar.

flow. In the present experiments, the gaseous flow rates were usually 3.0 ml/sec, and this means that the residence time of a gas in the reactor was less than 1.0 sec.

The gases employed were Ar, CO_2, and their mixtures, and they were purified before use. Ar passed through a Hydrox purifier to eliminate any water or oxygen. Carbon dioxide was passed through tubing cooled in a refrigerator in order to remove water. The silica employed here was Cabosil (H-5) silica powder, and it was prepared as round disk with 1 cm^2 area at around 1000 pounds force.

The sample was heated at various temperatures before the experiments in order to vary its surface OH state. Usually, the infrared spectrum of OH groups on SiO_2 was resolved to two or more bands. To obtain the areas of OH in the spectrum, a curve resolver-310 (DuPont) was used with the assumption that the curves were Gaussian.

RESULTS

The typical infrared spectrum of adsorbed CO_2 on SiO_2 preheated at 150°C

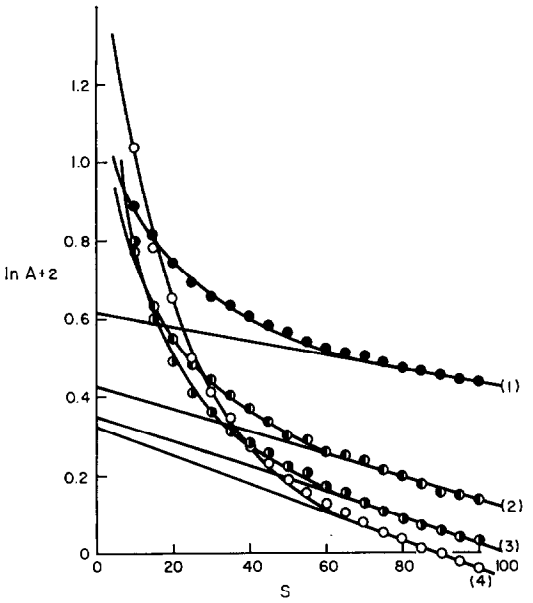

FIG. 3. The changes in optical density of adsorbed CO_2 during its desorption at 31°C from SiO_2 surfaces varied by heat treatment: (1) CO_2 desorption from the original SiO_2; (2) CO_2 desorption from SiO_2 preheated at 150°C; (3) CO_2 desorption from SiO_2 preheated at 200°C; (4) CO_2 desorption from SiO_2 preheated at 350°C. CO_2 was 100 kPa. The A_1^0 and k_1 for A_1 species obtained from these results were as follows: (1) A_1^0 0.2491, k_1, 1.76×10^{-3} sec^{-1}; (2) A_1^0 0.2060, k_1, 2.13×10^{-3} sec^{-1}; (3) A_1^0 0.1930, k_1, 3.30×10^{-3} sec^{-1}; (4) A_1^0 0.1864, k_1, 3.55×10^{-3} sec^{-1}.

is shown in Fig. 1. Gaseous CO_2 at 31°C was passed over the solid until equilibrium was reached, and then the flow was switched to Ar. The changes in the spectrum of the OH groups caused by CO_2 addition are also shown in Fig. 1. The infrared spectrum of surface OH groups on SiO_2 changed depending on heat treatment, as is shown in Fig. 2. The spectrum could be roughly separated to two parts: one is a sharp band, and its maximum absorption is observed at 3750 cm^{-1}; the other is broad, centered at around 3550 cm^{-1}. These bands were resolved, and their areas were obtained by means of the curve resolver. Their areas were normalized to the area of the total OH groups of the original SiO_2. The results are listed in Table 1.

Figure 3 represents the changes in the absorbance of adsorbed CO_2 on SiO_2 during desorption from surfaces of varying OH distribution controlled by heat treatment. For adsorption, 100 kPa CO_2 was used. In Fig. 3, the ordinate is expressed in terms of the logarithm of the absorbance. The curves in Fig. 3 could not be explained by any adsorption/desorption equations thus far proposed for single adsorbed species. Moreover, the curves in Fig. 3 intersect one another, which seems to indicate that there is more than one kind of adsorbed CO_2 on the SiO_2 surface.

All curves in Fig. 3 become straight lines after approximately 60 sec. These straight lines can be considered as the contribution from one of two adsorbed species, called the A_1 species. As is shown in Fig. 3, the value of A_1^0, which represents the absorbance of the A_1 species at time zero, was obtained for each curve by extrapolation.

By the subtraction of the absorbance of the A_1 species from the original one,

TABLE 1

Area of Absorption Peaks of OH Groups in the Spectrum[a]

Run	Preheat temperature (°C)	Total OH	Isolated OH	Bonded OH
1	Original	100.0	11.0	89.0
2	150	75.0	15.0	60.0
3	200	60.0	15.6	44.4
4	350	36.7	16.1	20.6

[a] Areas are normalized to total OH of the original silica.

the absorbance of the other adsorbed species (called A_2) was calculated. These values are given in Fig. 4. The absorbances in Fig. 4 are also linear with reaction time, and A_2^0 values were obtained for each curve in the same manner.

In Fig. 5, the relationship between the spectral area of OH groups at 3750 cm^{-1} and A_2^0 and between that of OH groups centered at 3550 cm^{-1} and A_1^0 are shown for each heat treatment of SiO_2.

For silica which was preheated at 150°C for 5 hr with Ar, the adsorption isotherms were obtained at 31, 42, 53, and 69°C for both the A_1 and A_2 species of adsorbed CO_2. The results are given in Fig. 6. To obtain the isotherms, A_1^0 and A_2^0 were measured by using 20 kPa through 100 kPa CO_2 at each adsorption temperature (see Figs. 7 and 8).

From the results shown in Fig. 6, the isosteric heats of adsorption were calculated for both species and are shown in Fig. 9. The activation energies for desorption were

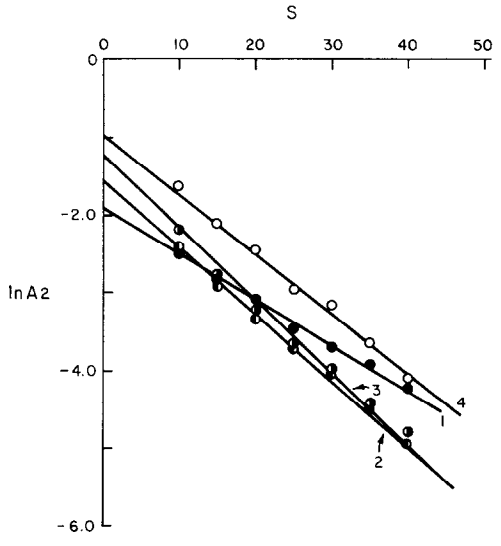

FIG. 4. A_2 type adsorbed CO_2 desorption at 31°C from various SiO_2 surfaces; symbols are the same as in Fig. 3. A_2^0 and k_2 were obtained for the A_2 species were as follows: (1) A_2^0, 0.1496, k_2, 5.83×10^{-2} sec^{-1}; (2) A_2^0, 0.2122, k_2, 8.55×10^{-2} sec^{-1}; (3) A_2^0, 0.2982, k_2, 9.30×10^{-2} sec^{-1}; (4) A_2^0, 0.3791, k_2, 7.75×10^{-2} sec^{-1}.

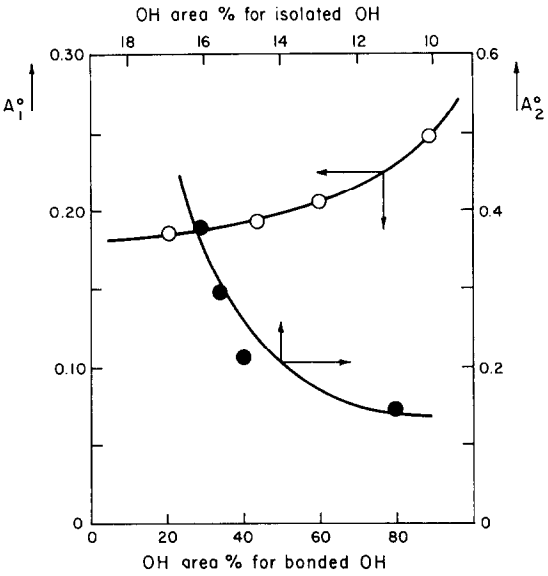

FIG. 5. The relationship between the isolated or bonded OH groups on SiO_2 and the optical density: (○) A_1 species; (●) A_2 species.

also calculated for both CO_2 adsorbed species by using their desorption rate constants obtained from Figs. 7 and 8, and the values are given in Fig. 10.

There were no significant changes in the infrared spectrum in the region 2000 through 1000 cm^{-1} during the adsorption and the desorption of CO_2 on SiO_2, which is evidence that no CO_3^{2-} ion was formed by the addition of CO_2 to SiO_2.

Finally, in the spectra, there was only one band assigned to the molecular-type adsorbed CO_2, but its behavior during the desorption was explained by the assumption that this band represented two kinds of adsorbed species. The position of the absorption maximum changed very little; for the original silica it was at 2347 cm^{-1}, and for the silica preheated at 350°C it was 2344 cm^{-1}.

DISCUSSION

Carbon dioxide adsorbs in Al_2O_3 and silica-alumina to form carbonate ions and molecular-type adsorbed CO_2. On the surface of SiO_2, however, no carbonate ion

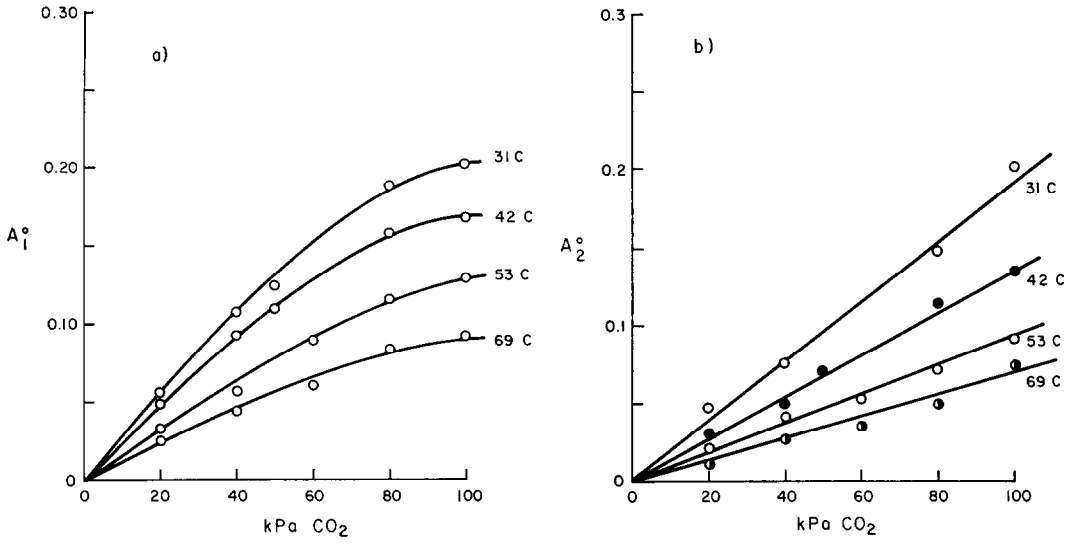

FIG. 6. (a) Adsorption isotherm for A_1 species. (b) Adsorption isotherm for A_2 species.

was observed by infrared spectroscopy when CO_2 was added over SiO_2 at 31 to 69°C. Infrared spectra showed only adsorbed molecular CO_2 associated with changes in the band shape of the hydroxyl groups on SiO_2. The hydroxyl groups showed a sharp band at 3750 cm^{-1} and a broad band centered at 3550 cm^{-1}. The latter band changed its band shape after exposure to CO_2.

We assumed that the OH groups on SiO_2 could be roughly separated into two groups—one isolated and the other bonded. The desorption of carbon dioxide from both OH groups is assumed to obey a first-order rate expression. Since for any adsorbed species the absorbance A_i can be assumed to be proportional to the partial coverage θ_i, the first-order expression for desorption is $-dA_i/dt = k_iA_i$. By these assumptions, the desorption curves for CO_2 on SiO_2 are well explained.

The amounts of OH groups can be controlled by heating the sample at the different temperatures. With increasing heating temperature, the amount of the bonded OH groups decreased, whereas that of the isolated OH groups increased, up to 350°C. Parkyns (*19*) also reported the same results using Al_2O_3. When Al_2O_3 was heated higher than 600°C, the amount of the isolated OH also began to decrease. The amounts of CO_2 adsorbed at equilibrium (expressed by its absorbance A_i^0), were proportional to the amounts of OH groups available, in both cases.

To discuss the thermodynamic properties of adsorbed CO_2 on the isolated OH and on the bonded OH groups, their adsorption isotherms and activation energies were obtained for the surface OH states of SiO_2. This was done by heating at 150°C for 5 hr in flowing Ar. The isosteric heats of CO_2 adsorption did not depend on the surface coverage. The adsorption isotherms seem to obey Henry's law for adsorption, and this means that the equilibrium constants for their adsorption are very small because of their small surface coverages. According to Eischens (*14*), the surface coverage of CO_2 on SiO_2 should be less than 0.1%. Peri (*15*) also reported a Henry-type adsorption isotherm for CO_2 on Aerosil silica.

The activation energies for desorption were very close to the isosteric heats of adsorption, so that their activation energies for adsorption should be almost zero.

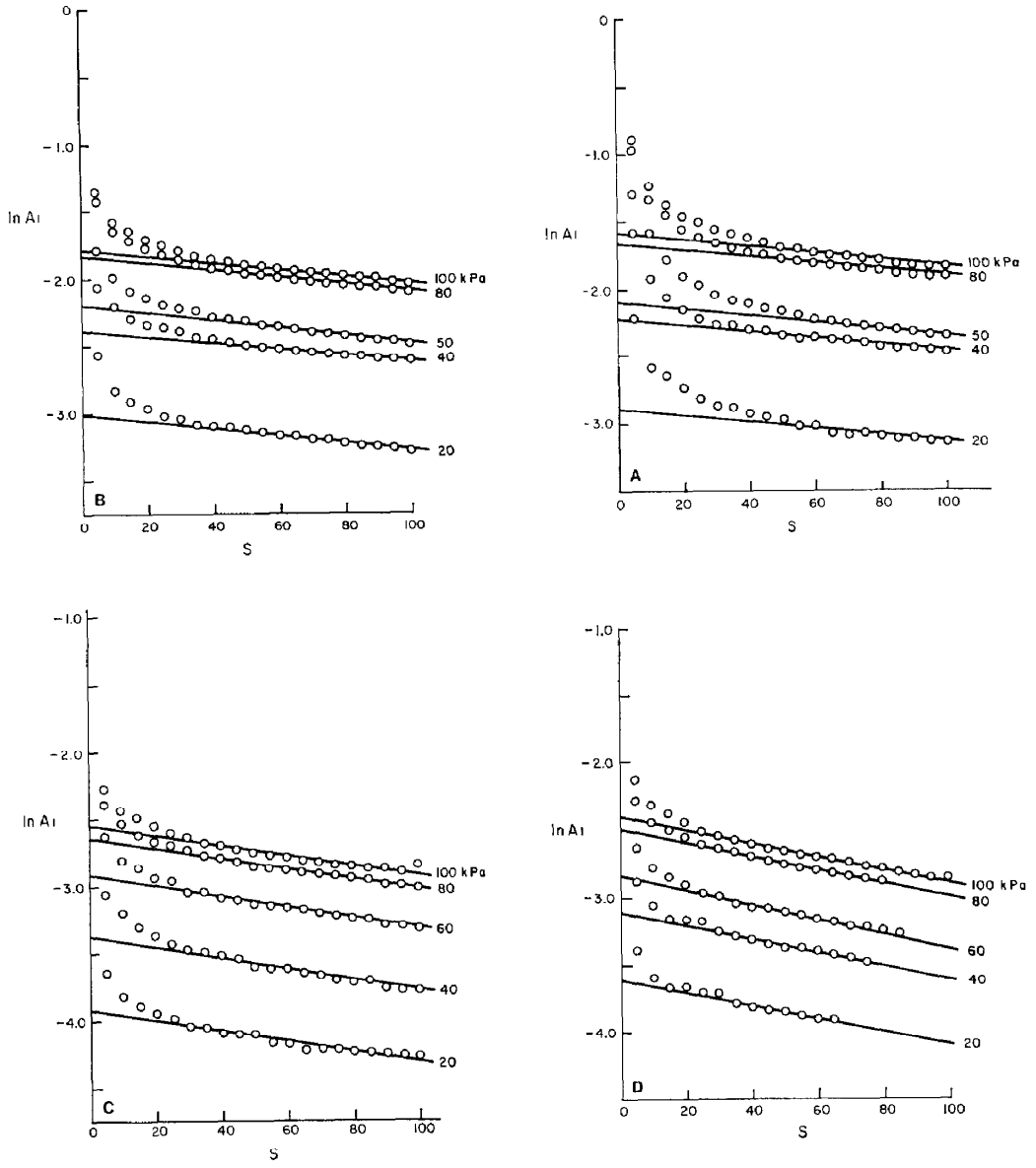

FIG. 7. CO_2 desorption for A_1 species. (A) Desorption at 31°C. A_1^0 and k_1 values as follows: (100 kPa) A_1^0, 0.2021, k_1, 2.26 × 10^{-3} sec^{-1}; (80 kPa) A_1^0, 0.1875, k_1, 2.16 × 10^{-3} sec^{-1}; (50 kPa) A_1^0, 0.1224, k_1, 2.30 × 10^{-3} sec^{-1}; (40 kPa) A_1^0, 0.1082, k_1, 2.25 × 10^{-3} sec^{-1}; (20 kPa) A_1^0, 0.0557, k_1, 2.11 × 10^{-3} sec^{-1}. Average k_1, 2.21 × 10^{-3} sec^{-1}. (B) Desorption at 42°C. A_1^0 and k_1 values as follows: (100 kPa) A_1^0, 0.1670, k_1, 2.40 × 10^{-3} sec^{-1}; (80 kPa) A_1^0, 0.1584, k_1, 2.33 × 10^{-3} sec^{-1}; (50 kPa) A_1^0, 0.1122, k_1, 2.75 × 10^{-3} sec^{-1}; (40 kPa) A_1^0, 0.0919, k_1, 2.28 × 10^{-3} sec^{-1}; (20 kPa) A_1^0, 0.0490, k_1, 2.60 × 10^{-3} sec^{-1}. Average k_1, 2.47 × 10^{-3} sec^{-1}. (C) CO_2 desorption at 53°C. A_1^0 and k_1 values as follows: (100 kPa) A_1^0, 0.1287, k_1, 3.70 × 10^{-3} sec^{-1}; (80 kPa) A_1^0, 0.1164, k_1, 3.70 × 10^{-3} sec^{-1}; (60 kPa) A_1, 0.0885, k_1, 3.90 × 10^{-3} sec^{-1}; (40 kPa) A_1^0, 0.0564, k_1, 3.95 × 10^{-3} sec^{-1}; (20 kPa) A_1^0, 0.0325, k_1, 3.90 × 10^{-3} sec^{-1}. Average k_1, 3.83 × 10^{-3} sec^{-1}. (D) Desorption at 69°C. A_1^0 and k_1 values as follows: (100 kPa) A_1^0, 0.0918, k_1, 4.92 × 10^{-3} sec^{-1}; (80 kPa) A_1^0, 0.0832, k_1, 4.93 × 10^{-3} sec^{-1}; (60 kPa) A_1^0, 0.0590, k_1, 5.40 × 10^{-3} sec^{-1}; (40 kPa) A_1^0, 0.0450, k_1, 5.00 × 10^{-3} sec^{-1}; (20 kPa) A_1^0, 0.0273, k_1, 4.85 × 10^{-3} sec^{-1}. Average k_1, 5.02 × 10^{-3} sec^{-1}.

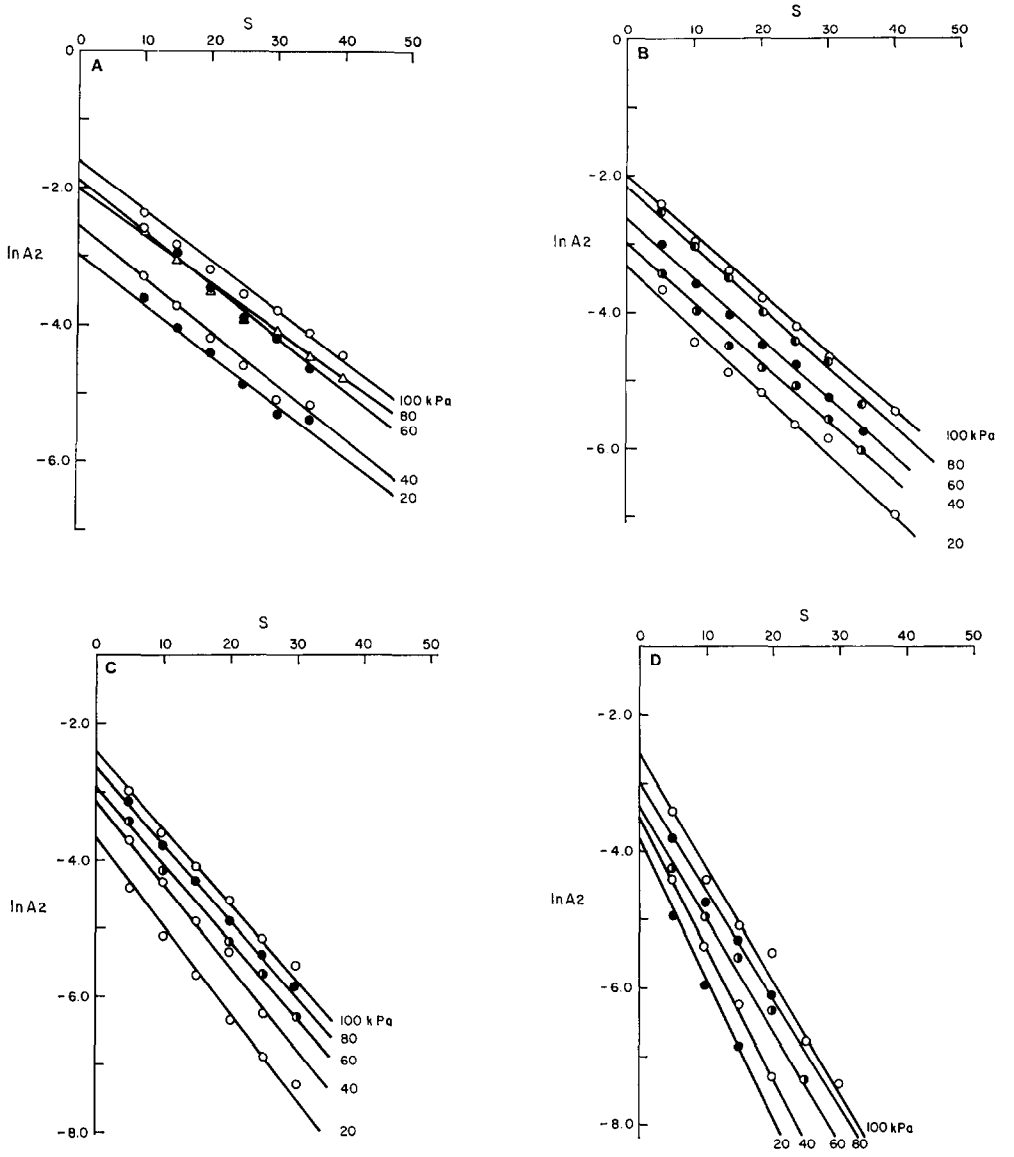

FIG. 8. CO_2 desorption for A_2 species. (A) Desorption at 31°C. A_2^0 and k_2 as follows: (100 kPa) A_2^0, 0.2019, k_2, 7.25 × 10^{-2} sec^{-1}; (80 kPa) A_2^0, 0.1496, k_2, 7.63 × 10^{-2} sec^{-1}; (50 kPa) A_2^0, 0.1353, k_2, 6.88 × 10^{-2} sec^{-1}; (40 kPa) A_2^0, 0.0781, k_2, 7.75 × 10^{-2} sec^{-1}; (20 kPa) A_2^0, 0.0498, k_2, 7.30 × 10^{-2} sec^{-1}. Average k_2, 7.36 × 10^{-2} sec^{-1}. (B) Desorption at 42°C. A_2^0 and k_1 values as follows: (100 kPa) A_2^0, 0.1327, k_2, 8.45 × 10^{-2} sec^{-1}; (80 kPa) A_2, 0.1142, k_2, 8.75 × 10^{-2} sec^{-1}; (50 kPa) A_2^0, 0.0706, k_2, 8.63 × 10^{-2} sec^{-1}; (40 kPa) A_2^0, 0.0498, k_2, 8.63 × 10^{-2} sec^{-1}; (20 kPa) A_2^0, 0.0351, k_2, 9.13 × 10^{-2} sec^{-1}. Average k_2, 8.72 × 10^{-2} sec^{-1}. (C) CO_2 desorption at 53°C. A_2^0 and k_2 values as follows: (100 kPa) A_2^0, 0.0907, k_2, 11.17 × 10^{-2} sec^{-1}; (80 kPa) A_2^0, 0.0707, k_2, 11.23 × 10^{-2} sec^{-1}; (60 kPa) A_2^0, 0.0523, k_2, 11.17 × 10^{-2} sec^{-1}; (40 kPa) A_2^0, 0.0429, k_2, 12.10 × 10^{-2} sec^{-1}; (20 kPa) A_2^0, 0.0247, k_2, 12.77 × 10^{-2} sec^{-1}. Average k_2, 11.69 × 10^{-2} sec^{-1}. (E) CO_2 Desorption at 69°C. A_2^0 and k_2 values as follows: (100 kPa) A_2^0, 0.0773, k_2, 16.48 × 10^{-2} sec^{-1}; (80 kPa) A_2^0, 0.0498, k_2, 15.80 × 10^{-2} sec^{-1}; (60 kPa) A_2^0, 0.0354, k_2, 17.20 × 10^{-2} sec^{-1}; (40 kPa) A_2^0, 0.0293, k_2, 18.78 × 10^{-2} sec^{-1}; (20 kPa) A_2^0, 0.0224, k_2, 20.05 × 10^{-2} sec^{-1}. Average k_2, 17.67 × 10^{-2} sec^{-1}.

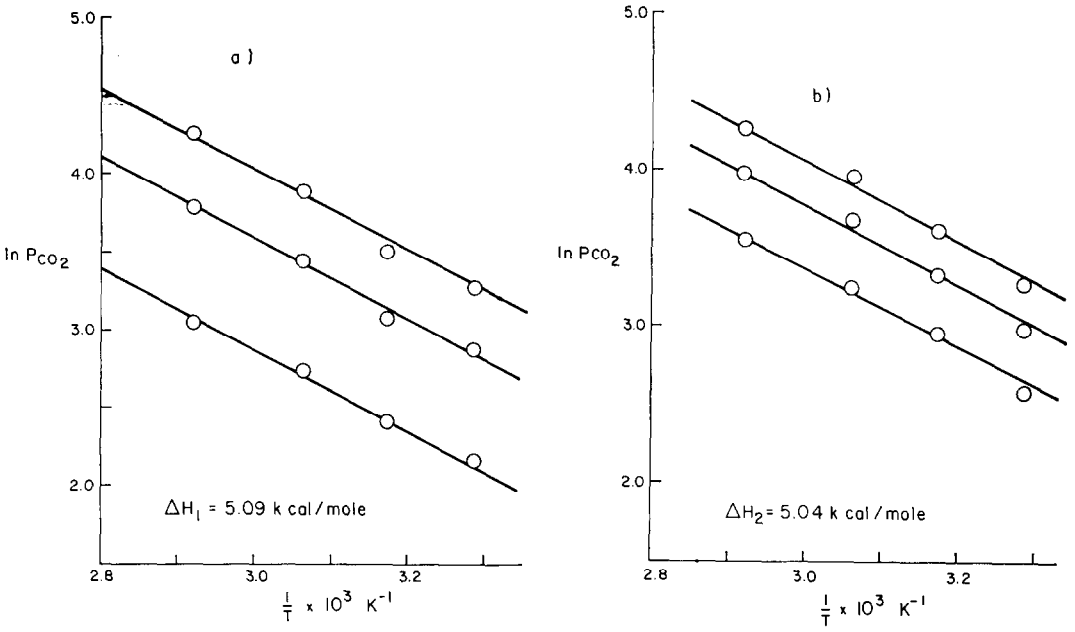

FIG. 9. (a) Isosteric heats of adsorption for A_1 species; lines were obtained from Fig. 6a at A_1^0 = 0.025, 0.050, and 0.075, respectively. (b) Isosteric heats of adsorption for A_2 species; lines were obtained from Fig. 6b at A_2^0 = 0.025, 0.0375, and 0.05, respectively.

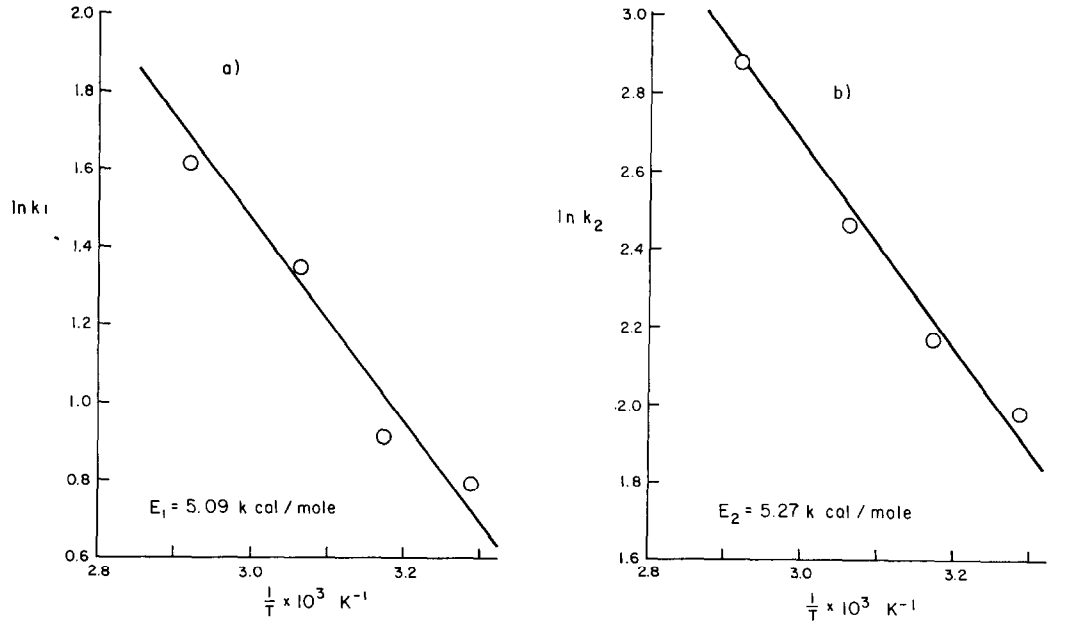

FIG. 10. (a) Activation energy for A_1 type CO_2 desorption. (b) Activation energy for A_2 type CO_2 desorption.

TABLE 2

Differences of the Standard Entropy Changes for Adsorption of A_1 and A_2 Species at Various Partial Pressures of CO_2 and Various Temperatures[a]

pCO_2 (kPa)	Standard entropy change[a] (cal/mol-°K)			
	31°C	42°C	53°C	69°C
100	−0.30	−0.46	−0.70	−0.34
80	−0.45	−0.65	−0.99	−1.02
60	—	—	−1.05	—
50	+0.20	−0.92	—	—
40	−0.65	−1.22	−0.55	−0.85
20	−0.22	−0.67	−0.55	−0.39

[a] $\Delta(\Delta S^0) = (-\Delta S_1^0) - (-\Delta S_2^0)$.

This result, however, does not mean necessarily that CO_2 adsorbs on SiO_2 in a form of physisorption. Chemisorptions with very small activation energies have been observed (*23*, *24*). On the contrary, CO_2 adsorption on SiO_2 seems to be chemisorption because of the observation of the infrared absorption band due to adsorbed CO_2 at temperatures up to 69°C. Carbon dioxide chemisorption on SiO_2 could be explained by considering the hydrogen bonding formed between CO_2 and OH groups on SiO_2. The observed heats of adsorption were around 5 kcal/mol for both types of CO_2 adsorbed, and these values are compatible with hydrogen bonding.

Although the activation energies for desorption and adsorption and the isosteric heats of adsorption were almost the same for CO_2 adsorbed on the isolated OH and on the bonded OH groups, the surface coverages (preexponential factors) for the two types of CO_2 on SiO_2 were different. This seems to indicate a difference in entropy between the A_1 and A_2 species.

The standard molar entropy change caused by adsorption at temperature T and equilibrium pressure P is given by:

$$-\Delta S^0 = -R \ln \frac{\theta P^0}{(1-\theta)P} - \frac{\Delta H^0}{T}, \quad (1)$$

where P^0 is the standard pressure (100 kPa) and ΔH^0 is equal to the isosteric heat of adsorption obtained (since it did not depend on the surface coverage). In the present experiments, θ is considered small enough to be neglected with respect to unity. Accordingly, the following equation can be obtained from Eq. (1):

$$-\Delta S^0 = -R \ln \left(\frac{\theta}{P} 10^2\right) - \frac{\Delta H}{T}. \quad (2)$$

The surface coverage θ could not be calculated from the present results, but it can be assumed that the absorbance of the infrared adsorption band is proportional to the surface coverage; i.e., $A = \alpha\theta$. Equation (2) then becomes:

$$-\Delta S^0 = -R \ln \left(\frac{A}{\alpha P} 10^2\right) - \frac{\Delta H}{T}. \quad (3)$$

Accordingly, the changes in the standard molar entropy for the A_1 and A_2 species can be obtained in terms of α by using the results for A_i^0 and ΔH_i. In the present work, the ΔH values for the A_1 and A_2 species are almost the same, so the difference of ΔS_0 between the formation of the A_1 and A_2 species can be obtained as follows:

$$\Delta(\Delta S^0) = (-\Delta S_1^0) - (-\Delta S_2^0) = -R \ln (A_1^0/A_2^0). \quad (4)$$

The calculated results are given in Table 2.

At all temperatures and pressures employed in this experiment except one, the sign of $\Delta(\Delta S^0)$ is always minus. This means the decrease of the entropy for CO_2 adsorption on isolated OH group is larger than that for CO_2 adsorbed on bonded OH groups. This seems reasonable because CO_2 adsorbed on isolated OH groups should be immobile, whereas CO_2 on bonded OH should be rather mobile, as is shown in the following scheme.

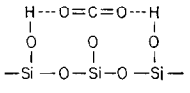

A_2 Species

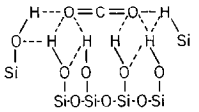

A_1 Species

The A_1 species has many possible modes of hydrogen bonding compared to the A_2 species, which leads to a higher entropy for the former.

ACKNOWLEDGMENTS

The financial support of NSF Grant ENG 72-04165 is gratefully acknowledged.

REFERENCES

1. McDonald, R. S., *J. Amer. Chem. Soc.* **79**, 850 (1957).
2. Peri, J. B., *J. Phys. Chem.* **69**, 220 (1965).
3. Jackson, P., and Parfitt, G. D., *J. Chem. Soc. Faraday I* **68**, 896 (1972).
4. Yates, D. J. C., *J. Phys. Chem.* **65**, 746 (1961).
5. Jacobs, P. A., van Cauwelaert, F. H., and Vansant, E. F. *J. Chem. Soc. Faraday I* **69**, 2130 (1973).
6. Peri, J. B., Paper presented at the 2nd Int. Congr. of Catalysis, Paris, 1960.
7. McDonald, R. S., *J. Phys. Chem.* **62**, 1168 (1958).
8. Folman, M., and Yates, D. J. C., *Proc. Roy. Soc. Ser. A* **246**, 32 (1958).
9. Basila, M. R., *J. Phys. Chem.* **66**, 2223 (1962).
10. Rosynek, M. P., *J. Phys. Chem.* **75**, 526 (1971).
11. Little, L. H., and Amberg, C. H., *Canad. J. Chem.* **40**, 1997 (1962).
12. Blyholder, G., and Neff, L. D., *J. Phys. Chem.* **66**, 1464 (1962).
13. O'Neill, C. E., and Yates, D. J. C., *Spectrochim. Acta* **17**, 953 (1961).
14. Eischens, R. P., and Pliskin, W. A., *in* "Advances in Catalysis," Vol. 9, p. 662. Academic Press, New York, 1957.
15. Peri, J. B., *J. Phys. Chem.* **70**, 3168 (1966).
16. Force, E. L., and Bell, A. T., *J. Catal.* **38**, 440 (1975).
17. Conner, W. C., and Bennett, C. O., *J. Catal.* **41**, 30 (1976).
18. Peri, J. B., *J. Phys. Chem.* **79**, 1582 (1975).
19. Parkyns, N. D., *J. Phys. Chem.* **75**, 526 (1971).
20. Kobayashi, M., and Kobayashi, H., *J. Catal.* **27**, 100 (1972).
21. Bennett, C. O., *AICHE J.* **13**, 890 (1967).
22. Ueno, A., Hochmuth, J. K., and Bennett, C. O., *J. Catal.* **49**, 225 (1977).
23. Wagener, S., *J. Phys. Chem.* **60**, 567 (1956); *ibid.*, **61**, 267 (1957).
24. Matsuda, A., *J. Res. Inst. Catal. Hokkaido Univ.* **5**, 71 (1957).